Electronic Supporting Information

Novel superwetting nanofibrous skins for removing stubborn soluble oil in emulsified wastewater

Xiangyu Li,[‡a] Qilin Gui,[‡b] Yen Wei [a] and Lin Feng*[a]

[a] *Department of Chemistry, Tsinghua University, Beijing, 100084, P. R. China*

[b] *Aerospace Research Institute of Materials and Processing Technology, Beijing, 100074, P. R. China*

[‡] *These authors contributed equally to this work.*

**Corresponding author, E-mail: fl@mail.tsinghua.edu.cn*

The PDF file includes:

Supplementary Figures

Fig. S1 The vernier caliper measurement of the substrate, indicating that the membrane thickness is about 150 μm.

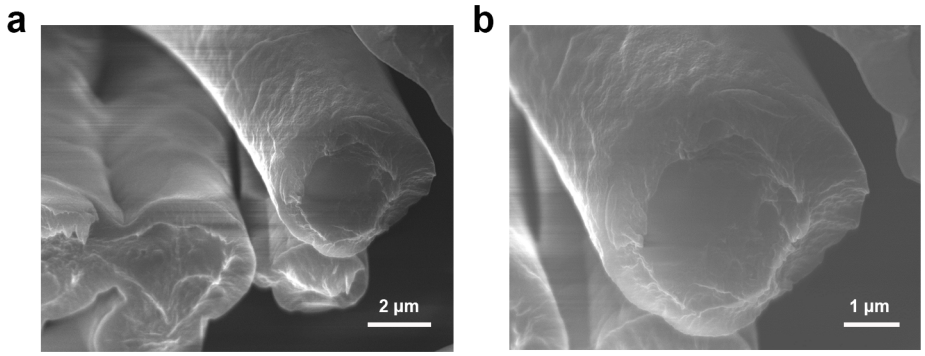

Fig. S2 (a) Low-magnification and (b) high-magnification cross-sectional SEM images of the PNVF@PPM, indicating the successful coverage of the PNVF skin layer on the membrane surface.

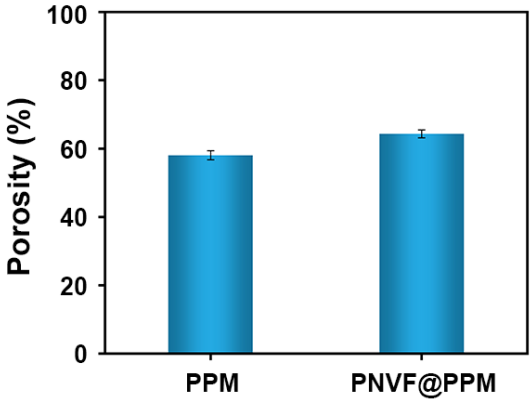

Fig. S3 Porosity (ε) of the PPM and PNVF@PPM. The values were measured by using n-butanol uptake tests according to the following equation ($\varepsilon(\%) = \frac{M_{BuOH} / \rho_{BuOH}}{(M_{BuOH} / \rho_{BuOH}) + (M_m / \rho_{PNVF})} \times 100\%$, where M_{BuOH} represents the n-butanol mass absorbed by the testing membrane, ρ_{BuOH} is the density of n-butanol, M_m is the mass of the sufficiently dried membrane, and ρ_{PNVF} is the density of the grafting PNVF).[1,2]

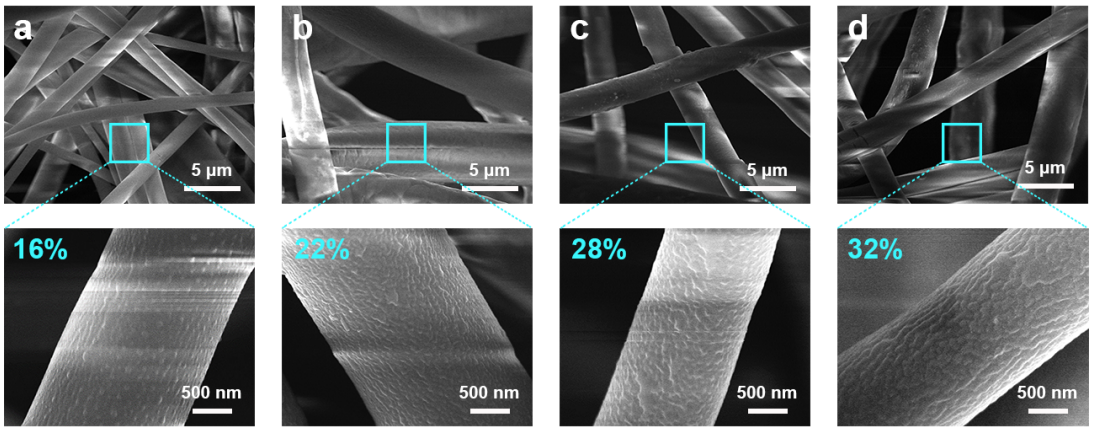

Fig. S4 Low and high-magnification SEM images of the obtained PNVF@PPMs with different grafting ratios of (a) 16%, (b) 22%, (c) 28%, and (d) 32%, respectively.

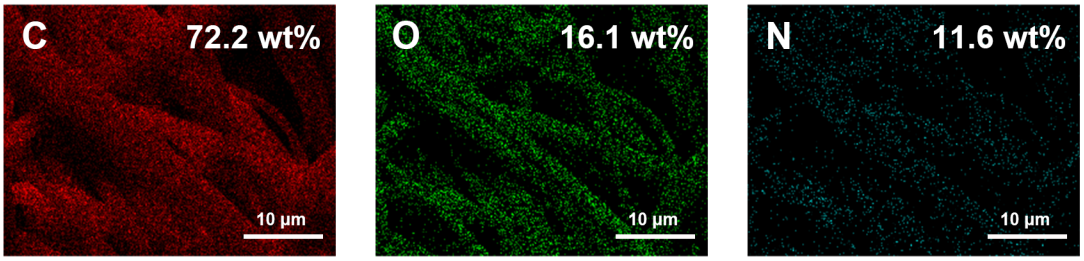

Fig. S5 Atomic concentration of PNVF@PPM. The EDX mapping clearly discerns the additional presence of O and N elements compared with the PPM substrate.

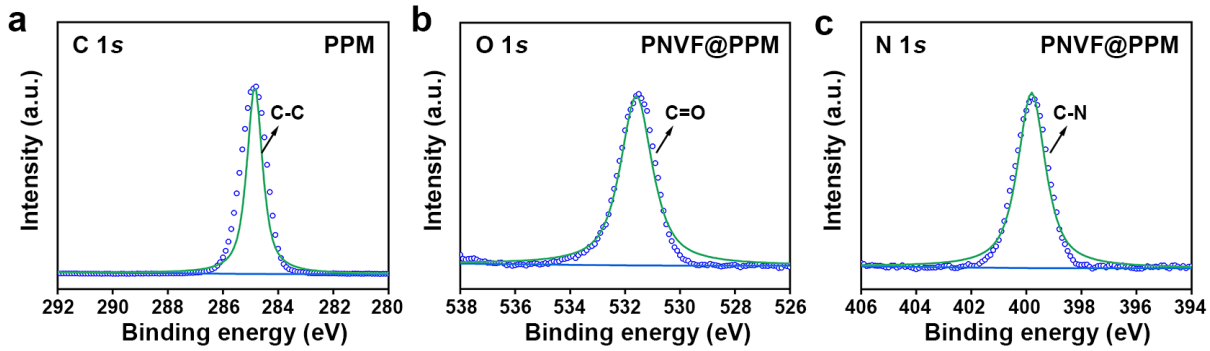

Fig. S6 High-resolution XPS spectra for different elements of the membrane before and after the modification. (a) The high-resolution XPS spectrum of C 1*s* for the pristine PPM, indicating the sole C-C moiety on the surface. The high-resolution XPS spectra of (b) O 1*s* and (c) N 1*s* spectra for PNVF@PPM showing the C=O and C-N moieties on the surface layer, respectively.

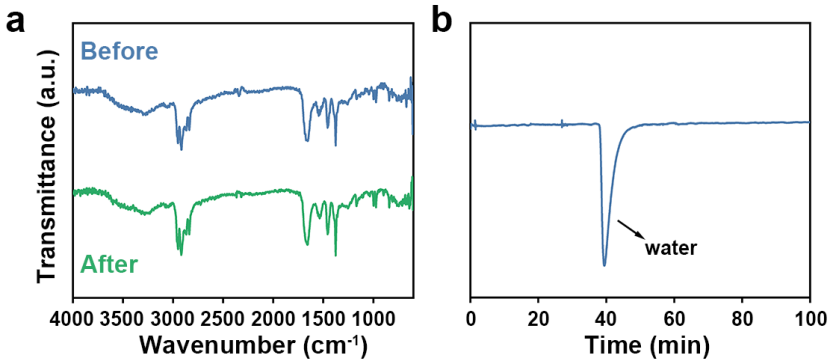

Fig. S7 The water resisting property of the PNVF@PPM. (a) FTIR spectra of the PNVF@PPM before and after water immersion for three days. (b) GPC measurement of the remaining water after the above treatment, indicating that no PNVF from the membrane falls off and dissolves in the water.

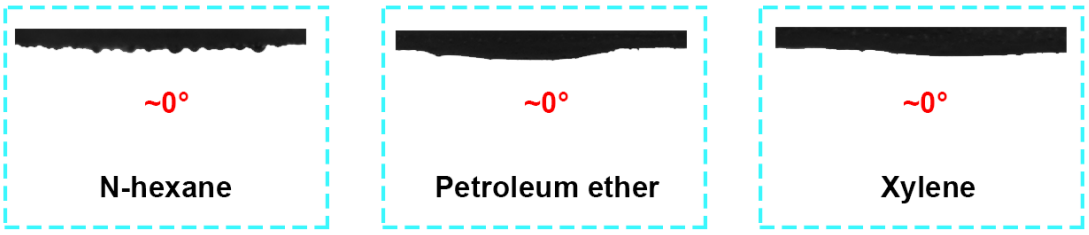

Fig. S8 The underwater oil wettability of the pristine PPM, indicating the superoleophilicity of the substrate.

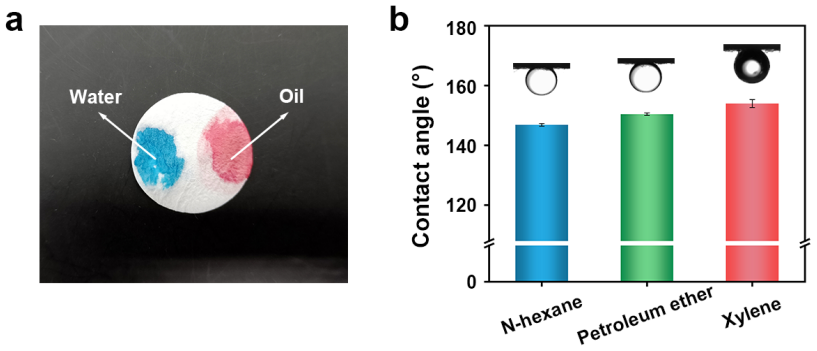

Fig. S9 Atmospheric durability tests of the PNVF@PPM. (a) Digital images of the water and oil (xylene) droplets on the membrane exposed to air for one month. (b) The corresponding underwater oil contact angles of the membrane after the treatment.

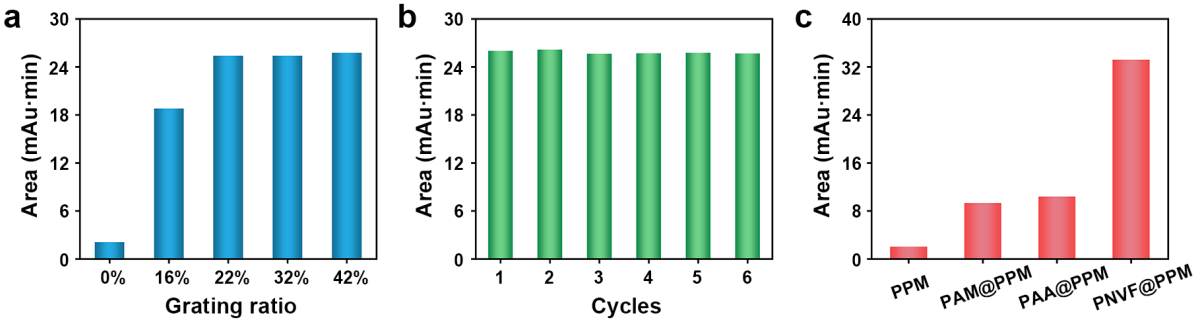

Fig. S10 The demonstration of adsorption performance of a series of membranes. (a) Adsorption capability of the PNVF@PPM with different grafting ratios for wastewater sample (xylene concentration at 200 mg L^{-1}). (b) Cyclic adsorption capability of the PNVF@PPM with 42% grafting ratios for wastewater sample. (c) Adsorption capability of the PNVF@PPM, PAA@PPM, and PAM@PPM (~40% grafting ratio of three kinds of membranes) for wastewater sample.

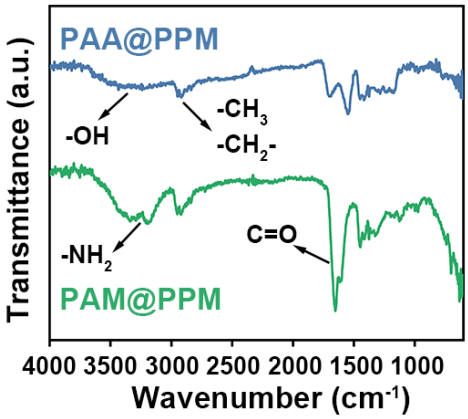

Fig. S11 FTIR spectra of the PAA@PPM and PAM@PPM. The broad peak at 3389 cm^{-1} ascribed to -OH verifies the existence of polyacrylic acid on the membrane surface. Likewise, the peaks at 3196 and 3342 cm^{-1} ascribed to $-NH_2$ symmetric and antisymmetric stretching vibration verify the polyacrylamide structure on the other membrane surface.

Fig. S12 Digital images of the sesame oil-in-water, petrol-in-water, diesel-in-water emulsions before and after the membrane separation.

Supplementary Tables

Table S1. Evaluation of the hydrophobicity of the grafting monomers.

Monomer	AA	AM	NVF
log $P^{(a)}$	-2.56	-0.56	0.53

[(a)] log *P* represents the oil-water partition coefficient to evaluate the hydrophobicity of the compounds. The data of log *P* were obtained from the SciFinder Database.

Table S2. Summary of the properties of the oils.

Oils[(a)]	Viscosity (mPa. s)	Density (g cm^{-3})	Surface tension (mN m^{-1})
N-hexane	0.3	0.66	18.8
Petroleum ether	0.3	0.66	18.4
Xylene	0.7	0.86	30.7
Sesame oil	52.5	0.92	28.1
Petrol	0.8	0.73	21.6
Diesel	2.9	0.84	26.8

[(a)] The data of the properties of the oils (at 20°C if unspecified) were obtained from the literature.

Table S3. Performance comparison of the PNVF@PPM with other recently reported filtration membranes for oil-in-water emulsion separation.

Membrane	Pressure	Emulsion type	Flux ($L\ m^{-2}\ h^{-1}$)	Separation efficiency	Residual oil content ($mg\ L^{-1}$)	Reference
Composite nanofibrous membrane	0.005 MPa	N-hexane-in-water	692	99.40%	23	3
ZNG-g-PVDF membrane	0.01 MPa	Isooctane-in-water	2500	99.80%	19	4
TiO_2@PSA/PAN membrane	0.01 MPa	N-hexane-in-water	3264	99.60%	40	5
GO/g-C_3N_4@TiO_2 membrane	0.05 MPa	Soybean oil-in-water	158	99.90%	/[a]	6
PVDF@PDA@SiO_2 membrane	0.08 MPa	Dichloroethane-in-water	458	99.91%	19	7
WBP@PBDF membrane	0.085 MPa	N-hexane-in-water	814	99.40%	75	8
PNIPAAm modified membrane	0.1 MPa	N-hexane-in-water	2200	99.30%	60	9
Lithium exchanged vermiculite membrane	0.1 MPa	N-hexane-in-water	6500	95.40%	/	10
GO/PG/CN@BOC membrane	~0.1 MPa	N-hexane-in-water	450	99.90%	/	11
Vitrimer epoxy resin membranes	~0.1 MPa	Heptane-in-water	1.36×10^7	98.00%	130	12
Hydrogel coated filter paper	Gravity	N-hexane-in-water	63	99.40%	/	13
PFOA@TiO_2 coated membrane	Gravity	Toluene-in-water	400	/	150	14
Reduced PK membrane	Gravity	Soybean oil-in-water	497	99.80%	20	15
NiCo-LDH/PVDF membrane	Gravity	Dichloroethane-in-water	600	99.70%	40	16
Three-dimensional attapulgite	Gravity	N-hexane-in-water	218	99.60%	60	17
SiO_2@PAN nanofibrous membrane	Gravity	N-hexane-in-water	1120	/	50	18
PNVF@PPM	**Gravity**	**N-hexane-in-water**	**1396**	**>99.99%**	**<0.5**	**This work**

[a] /: Not provided

Supplementary References

1. Y. Zhai, K. Xiao, J. Yu, J. Yang and B. Ding, *J. Mater. Chem. A*, 2015, **3**, 10551-10558.
2. M. Wu, W. Liu, P. Mu, Q. Wang and J. Li, *ACS Appl. Mater. Interfaces*, 2020, **12**, 53484-53493.
3. J. Ge, D. Zong, Q. Jin, J. Yu and B. Ding, *Adv. Funct. Mater.*, 2018, **28**, 1705051.
4. Y. Zhu, J. Wang, F. Zhang, S. Gao, A. Wang, W. Fang and J. Jin, *Adv. Funct. Mater.*, 2018, **28**, 1804121.
5. Z. Zhu, W. Wang, D. Qi, Y. Luo, Y. Liu, Y. Xu, F. Cui, C. Wang and X. Chen, *Adv. Mater.*, 2018, **30**, 1801870.
6. Y. Liu, Y. Su, J. Guan, J. Cao, R. Zhang, M. He, K. Gao, L. Zhou and Z. Jiang, *Adv. Funct. Mater.*, 2018, **28**, 1706545.
7. J. Cui, Z. Zhou, A. Xie, M. Meng, Y. Cui, S. Liu, J. Lu, S. Zhou, Y. Yan and H. Dong, *Sep. Purif. Technol.*, 2019, **209**, 434-442.
8. G. Shi, Y. Shen, P. Mu, Q. Wang, Y. Yang, S. Ma and J. Li, *Green Chem.*, 2020, **22**, 1345-1352.
9. W. Zhang, N. Liu, Q. Zhang, R. Qu, Y. Liu, X. Li, Y. Wei, L. Feng and L. Jiang, *Angew. Chem. Int. Ed.*, 2018, **57**, 5740-5745.
10. K. Huang, P. Rowe, C. Chi, V. Sreepal, T. Bohn, K.-G. Zhou, Y. Su, E. Prestat, P. Balakrishna Pillai, C.T. Cherian, A. Michaelides and R. R. Nair, *Nat. Commun.* 2020, **11**, 1097.
11. Y. Cai, D. Chen, N. Li, Q. Xu, H. Li, J. He and J. Lu, *Adv. Mater.*, 2020, **32**, 2001265.
12. C. Ye, V. S. D. Voet, R. Folkersma and K. Loos, *Adv. Mater.*, 2021, **33**, 2008460.
13. J. Fan, Y. Song, S. Wang, J. Meng, G. Yang, X. Guo, L. Feng and L. Jiang, *Adv. Funct. Mater.*, 2015, **25**, 5368-5375.
14. Y. Sun and Z. Guo, *Adv. Mater.*, 2020, **32**, 2004875.

15. L. Cheng, A. R. Shaikh, L.-F. Fang, S. Jeon, C.-J. Liu, L. Zhang, H.-C. Wu, D.-M. Wang and H. Matsuyama, *ACS Appl. Mater. Interfaces*, 2018, **10**, 44880-44889.
16. J. Cui, Z. Zhou, A. Xie, Q. Wang, S. Liu, J. Lang, C. Li, Y. Yan and J. Dai, *J. Membr. Sci.*, 2019, **573**, 226-233.
17. M. Cui, P. Mu, Y. Shen, G. Zhu, L. Luo and J. Li, *Sep. Purif. Technol.*, 2020, **235**, 116210.
18. J. Ge, J. Zhang, F. Wang, Z. Li, J. Yu and B. Ding, *J. Mater. Chem. A*, 2017, **5**, 497-502.